Hybrid UP-PWM for Single-phase transformerless photovoltaic inverter to improve Zero-Crossing Distortion

Zhongting Tang, Mei Su, Yao Sun, Hui Wang, Bin Guo
School of Information Science and Engineering,
Central South University
Changsha, China
TinaTCSU@163.com

Yunfan Yang
International Department,
Yali High School
Changsha, China
841912799@qq.com

***Abstract*—The zero-crossing distortion (ZCD) is a common problem in Single-phase transformerless photovoltaic (PV) inverter. By establishing the mathematical model of the HERIC type inverter which is proved to be a mainstream transformerless PV inverter, the result for causing the ZCD is presented. To suppressing the ZCD while achieve high efficiency and reactive power capability, a hybrid unipolar pulse width modulation (UP-PWM) is proposed. The proposed method adopts grid frequency unipolar pulse width modulation (GFUP-PWM) when outputting active power. While generating reactive power, the leg switches are all closed, and only the freewheeling switches work at high frequency. Aiming at reducing the ZCD, a modified high frequency unipolar pulse width modulation (HFUP-PWM) is proposed near the voltage and current zero-crossing point (ZCP) regions. And the duty cycle is adjusted to compensate the narrow pulse limit and dead zone in HFUP-PWM. The proposed scheme has high efficiency and good power quality while provide reactive power support. Finally, the effectiveness of the proposed modulation scheme is verified by the simulations results based on a 4-kW inverter at 20-kHz switching frequency.**

Keywords—dead zone, GFUP-PWM, HFUP-PWM, hybrid UP-PWM, narrow pulse limit, ZCD

I. INTRODUCTION (*HEADING 1*)

With the fast development of the residential renewable energy generation technology, the grid-connection inverter has been thoroughly researched in various fields, such as topologies, modulation strategies, control methods and so on [1]-[3]. Owing to the high power density, high efficiency and low cost, the transformerless inverter is a better alternative than the one with a transformer. However, the leakage current which must be suppressed to a certain level will be stimulated by the high-frequency common-mode voltage (CMV) [4]. Thus, various AC bypass topologies were proposed to suppress the leakage current, such as H5 topology [5], HERIC topology [6], and diverse H6 topologies [7]-[8].

The main stream transformerless PV inverter, HERIC type inverter, can supressing leakage current in any modulation scheme. Thus, in recently, the researches of modulation are almost aim at reactive power capability which is another serious function [9], [10], [12], [13]. According to the international standard VDE-AR-N4105, the adjustable range of power factor in power generation system or power generation unit is set from 0.9 leading to 0.9 lagging [13]. In [9], a combined unipolar and bipolar PWM is proposed to obtain reactive power capability. But, the switching losses are increased with BP-PWM. Thus, a modulation technique which can provide bidirectional path during freewheeling period to achieve reactive power capability and low switching losses is proposed for H5 and HERIC topologies in [10]. However, the zero-crossing distortion (ZCD) which effects on power quality has not been discussed.

The ZCD which can be divided into two kinds. According to literature [11], the ZCD at current ZCP is ascribed to the neglecting the inductor voltage which is an inherent problem of single-phase. Therefore, literature [12] shifts the phase angle of inverter output reference voltage to reduce the ZCD at current ZCP. However, the ZCD at voltage ZCP which is generated by the narrow pulse limit and dead zone hasn't been mentioned. Besides, the ZCD near both the current and voltage ZCP are also generated because the polarity of voltage and current are inaccuracy.

Thus, to take account of high efficiency, good quality and reactive power capability, this paper proposes a hybrid UP-PWM for HERIC type inverter. The proposed scheme consists of three modulation methods, e.i. GFUP-PWM, a modified HFUP-PWM and modulation for outing reactive power proposed in [10]. This paper is organized as follows: In Section 2, the conventional modulation schemes for HERIC type inverter are presented, and the ZCD problem is discussed. Then, the proposed hybrid modulation technique is introduced. What's more, it depicts how to improve the ZCD purely from modulation technique. Finally, the feasibility of the proposed modulation method is verified through simulation and experiment in Section 3, and the conclusions are drawn in Section 4.

II. PROPOSED MODULATION TECHNIQUES

The topology of HERIC type inverter is shown in Fig.1. U_{dc} is the DC link voltage, and i_g is the inductor current. The voltage equation of the grid-connected inverter is

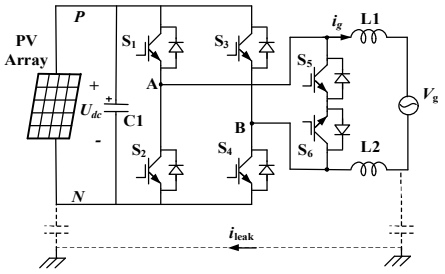

Fig. 1. Topology of HERIC type single-phase photovoltaic inverter

$$V_L(t)=L\frac{di_g(t)}{d_t}=V_{AB}(t)-V_g(t) \tag{1}$$

where $V_L(t)$ is the voltage increment across the filter inductor L (L=$L1$+$L2$). The $V_g(t)$ is the grid voltage, and $V_{AB}(t)$ is the differential-mode voltage (DMV) between terminal A to terminal B. The CMV V_{CM} and DMV V_{DM} are defined as

$$V_{CM}=\frac{V_{AN}+V_{BN}}{2} \tag{2}$$

$$V_{DM}=V_{AB}=V_{AN}-V_{BN} \tag{3}$$

where V_{AN} and V_{BN} are the voltages of terminals A and B to terminal N.

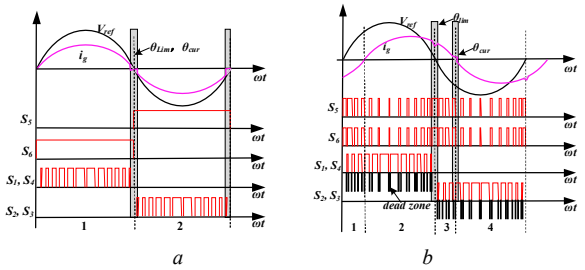

a b

Fig. 2. Conventional modulation schemes
a. GFUP-PWM
b. HFUP-PWM

Generally, the conventional UP-PWMs for HERIC type inverter include GFUP-PWM and HFUP-PWM as shown in Fig.2 (a) and (b), respectively. V_{ref} is the desiring output voltage. The operation principle of GFUP-PWM is shown in Fig.2 (a), where the freewheeling switches S_5 and S_6 work in grid frequency, while the leg switches $S_{1\text{-}4}$ work in high frequency. While, the HFUP-PWM is shown in Fig.2 (b). The leg switches $S_{1\text{-}4}$ and freewheeling switches $S_{5,6}$ work in high-frequency complementary. Taking into account the dead zone of power semiconductor switches, an extra dead state is added to the switchover process. In the GFUP-PWM, S_5 (S_6) and D_6 (D_5) are opened during generating reactive power. However, when S_1 (S_2) and S_4 (S_3) are opened in conduction mode, the short-circuited is occurred. Thus, the GFUP-PWM has no reactive operation condition. However, the HFUP-PWM can provide reactive power support because the $S_{1\text{-}4}$ and $S_{5,6}$ operate complementarily. And the insertion of dead zone ensures safety operation.

A. ZCD analysis

1) ZCD near the voltage ZCP

The ZCD near voltage ZCP is generated by the narrow pulse limit and dead zone. During one switching cycle, the duty cycle d is

$$V_{AB}=dU_{dc},\quad \frac{di_g(t)}{d_t}=\frac{dU_{dc}-V_g}{L} \tag{4}$$

The inverter keeps freewheeling mode if the duty cycle is less than narrow pulse limit.

$$d=\frac{L\frac{di_g}{dt}+V_g}{U_{dc}}<d_{\lim}=\frac{\theta_{\lim}f}{2\pi f_s} \tag{5}$$

where d_{lim} is the sum of the narrow pulse limit and the dead zone. For the sake of convenience in the computation, d_{lim} is replaced by θ_{lim}, f is the fundamental frequency and f_s is the switch frequency. Assuming $V_g(t)$=$V_m$sin(ωt), the derivative of current is

$$\frac{di_g(t)}{d_t}=\frac{-V_m\sin(\omega t)}{L} \tag{6}$$

Then, when d<d_{lim}, the current increment can be expressed as

$$\Delta i_g(t)=\int_{\pi-\theta_{\lim}/2}^{\pi}\frac{di_g(t)}{dt}dt=\frac{V_m}{\omega L}(\cos(\frac{\theta_{\lim}}{2})-1) \tag{7}$$

However, the desiring inductor current increment is

$$\Delta i_g^*(t)=\int_{\pi-\theta_{\lim}/2}^{\pi}\frac{di_g(t)}{dt}dt=\frac{dU_{dc}\theta_{\lim}}{4L\omega}+\frac{V_m}{\omega L}(\cos(\frac{\theta_{\lim}}{2})-1) \tag{8}$$

The actual voltage can't trace the reference and leads to current distortion. The expression of the current distortion is

$$\Delta i_{gerr}=\Delta i_g^*(t)-\Delta i_g(t)=\frac{dU_{dc}\theta_{\lim}}{4L\omega} \tag{9}$$

It is illustrated in formula (9) that the distortion Δi_{gerr} varies directly as θ_{lim}, while U_{dc}, L and ω are fixed parameters. The relation graph of Δi_{gerr} and θ_{lim} is drawn in Fig.3 (a) with the values of U_{dc}=360V, ω=100π, L=1.5mH. The ranges of θ_{lim} is 0~0.01π. It illustrates that Δi_{gerr} has similar trend with the change in θ_{lim}. And, the maximum distortion is at the end time of d<d_{lim}. Besides, the ZCD near voltage ZCP has no bearing on power factor.

2) ZCD near the current ZCP

Defining the current reference of inductor as $i_g^*(t)$=-I_m^*sin(ωt+φ), where φ is the power factor angle. When working at freewheeling mode, the derivative of i_g^* is

$$\frac{di_g^*(t)}{dt}=-\omega I_m^*\cos(\omega t+\varphi) \tag{10}$$

The drop velocity of i_g is smaller than that of i_g^*, when the derivative of i_g meet as

$$\left|\frac{di_g(t)}{dt}\right|<\left|\frac{di_g^*(t)}{dt}\right| \tag{11}$$

The ZCD is generated because the i_g can't trace the i_g^* any more. Substituting (10) and (11) to (4), the phase angle θ_{cur} of distortion region can be expressed as

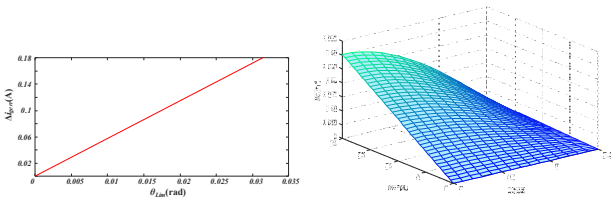

Fig. 3. ZCD relationship
a. Δi_{gerr} corresponding to θ_{lim}
b. θ_{cur} corresponding to I_m^* and φ

$$\theta_{cur} = -\operatorname{arccot}(-\frac{V_m}{\omega L I_m^* \cos\varphi} + \tan\varphi) \tag{12}$$

From the above formula, it is obviously that the distortion angle θ_{cur} is decided by the maximum value of gird voltage V_m, grid angle frequency ω, filter inductor L, the reference current I_m^* and φ. Among them , I_m^* is set through the power size of inverter, and φ is relate to the reactive power capability. The relation graph of θ_{cur}, I_m^* and φ is drawn in Fig. 3 (b) with the values of V_m=311V, ω=100π, L=1.5mH. The ranges of I_m^* and φ are 0~20A and 0~π/2, respectively. Fig. 3 (b) shows that θ_{cur} has similar trend with the change in I_m^*, while has reverse trend with the change in φ. Therefore, the larger the reference amplitude of the current is, the larger the distortion is.

As illustrated in Fig.2, the two ZCDs are existed in both GFUP-PWM and HFUP-PWM. Under GFUP-PWM in unity power factor, the ZCD angles θ_{lim} and θ_{cur} are always coincident, which is described in the grey part of Fig.2 (a). The more distinct distortion condition is depicted in the grey part of Fig.2 (b), where the inverter adopts HFUP-PWM in non-unity power factor.

B. Proposed hybrid UP-PWM

This paper proposed a hybrid UP-PWM technique for HERIC type inverter. The concrete operation principles as shown in Fig.4. When working under non-unity power factor, the operation region are divided into 8 kinds as shown in Fig.5 (b). There are three modulation kinds:

(1) GFUP-PWM: in region 3 and 7. The operation principle of GFUP-PWM can achieve low switching losses and ripple current.

(2) HFUP-PWM: in region 2, 4, 6 and 8. Due to the polarity uncertainty of output voltage and current, the HFUP-PWM can ensure safety operation of inverter.

(3) UP-PWM for generating reactive power: in region 1 and 5. To provide reactive power capability and reduce switching losses, this paper adopts a UP-PWM for generating reactive power. The operation principle is depicted in Fig.6. The leg switches $S_{1\text{-}4}$ are OFF in region 1 and 5, while the freewheeling switches $S_{5,6}$ operate in high frequency. The four operation modes are:

Mode1: At 5 region shown in Fig.4 (b), all switches are closed, the inverter works on reverse conduction mode. V_{AN}=V_P=0 and V_B=V_N=U_{dc}.

$$V_{CM} = \frac{0+U_{dc}}{2} = \frac{U_{dc}}{2} \tag{13}$$

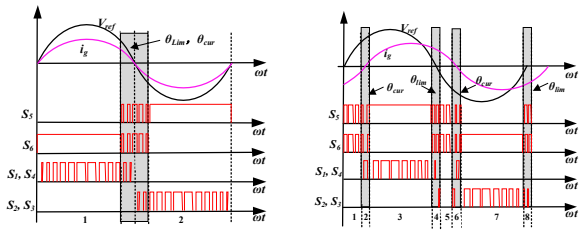

Fig. 4. Proposed hybrid UP-PWM
a unity power factor
b non-unity power factor

$$V_{DM} = 0 - U_{dc} = -U_{dc} \tag{14}$$

Mode2: At 5 region shown in Fig.4 (b), only S5 and S6 are open, the inverter works on freewheeling mode. V_{AN}=V_P=U_{dc}/2 and V_B=V_N=U_{dc} /2.

$$V_{CM} = \frac{U_{dc}/2 + U_{dc}/2}{2} = \frac{U_{dc}}{2} \tag{15}$$

$$V_{DM} = U_{dc}/2 - U_{dc}/2 = 0 \tag{16}$$

Mode7 At 1 region shown in Fig.4 (b), all switches are closed, the inverter works on forward conduction mode. V_{AN}=V_P=U_{dc} and V_B=V_N=0.

$$V_{CM} = \frac{U_{dc}+0}{2} = \frac{U_{dc}}{2} \tag{17}$$

$$V_{DM} = U_{dc} - 0 = U_{dc} \tag{18}$$

Mode8: At 1 region shown in Fig.4 (b), only S5 and S6 are open, the inverter works on freewheeling mode. V_{AN}=V_P=U_{dc}/2 and V_B=V_N=U_{dc} /2.

$$V_{CM} = \frac{U_{dc}/2 + U_{dc}/2}{2} = \frac{U_{dc}}{2} \tag{19}$$

$$V_{DM} = U_{dc}/2 - U_{dc}/2 = 0 \tag{20}$$

The formula (14), (16), (18) and (20) illustrate that the proposed modulation method has no leakage current problem when generating reactive power. The value of V_{DM} changes as the same as GFUP-PWM. Besides, it has no necessary to take consideration on the narrow pulse limit and dead zone in reactive power because there is no switchover operation of switches. When operating in unity power factor, there has no region 1 and 5. Therefore, there are just 2 operation modes as shown in Fig. 4 (a).

C. Revising HFUP-PWM to improve ZCD

This paper proposed a revising HFUP-PWM to compensate the ZCD which is caused by narrow pulse limit and dead zone. The region θ, which adopts HFUP-PWM must meet the follow condition.

$$\theta \geq \max(\theta_{\lim}, \theta_{cur}) \tag{20}$$

The principle of inserting dead zone is shown in Fig.5 (a), which is positive conduction mode. There are two dead zones in one switching frequency. When the inverter operation at

dead zone, VAB is equal to -U_{dc}. Then V_{AB} in one switching cycle time is expressed as

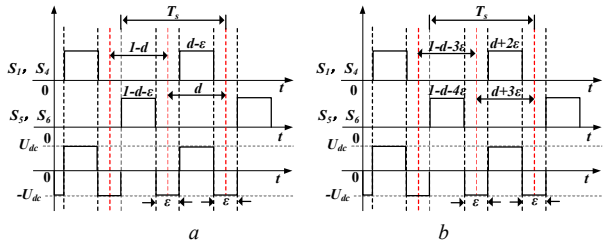

Fig. 5. Dead zone compensation
a. conventional compensation
b. revising compensation

$$V_{AB}|_{T_s} = (d-\varepsilon)U_{dc} + (1-d-\varepsilon)0 + 2\varepsilon(-U_{dc}) = (d-3\varepsilon)U_{dc} \quad (21)$$

where ε is the dead zone ratio, T_S is the switching cycle time. The output value of V_{AB} is less than the desired dU_{dc} when inserting dead zone. Therefore, to compensation the difference, the revising dead zone is described in Fig.7 (b). Due to the reverse voltage in dead zone, the duty cycle d should be revised to be d+3ε. The revising method can achieve V_{AB} as

$$V'_{AB}|_{T_s} = (d+2\varepsilon)U_{dc} + (1-d-4\varepsilon)0 + 2\varepsilon(-U_{dc}) = dU_{dc} \quad (22)$$

When the duty cycle d less than narrow pulse d_{nar}, d is equal to zero. Thus, the current can't trace the reference well. Tush, an artful handling is needed. The revising duty cycle is refine as D, D= d+3ε.

$$D = \begin{cases} D & , \quad D > d_{nar} \\ D + d_{plu}, & D \le d_{nar} \end{cases} \quad and \quad \varepsilon = \begin{cases} \varepsilon & , \quad D > d_{nar} \\ \varepsilon + d_{plu}/2, & D \le d_{nar} \end{cases} \quad (23)$$

where d_{plu} is the revising value which is longer than d_{nar} to ensure effective turn-on time.

Most of the time, the proposed hybrid UP-PWM method operates in grid frequency modulation. Only in the compensation range of ZCD, θ, the HFUP-PWM is realized. Therefore, the efficiency and ripple current of hybrid modulation scheme is close to the GFUP-PWM. The hybrid UP-PWM combines the advantages of the three modulation methods to achieve low switching losses, good power quality and reactive power capability.

D. Comparison of switching losses

The semiconductor power losses are consist of conduction losses and switching losses. The conduction losses has little relationship with modulation strategy. However, different modulation methods can lead to different switching losses. As discussed in [14], the switching losses are produced in insulated gate bipolar transistor (IGBT) and anti-parallel body diode.

$$P_{SW} = (P_M + P_D) = f_s\left((E_{onM} + E_{offM}) + E_{onD}\right)\frac{V_{ce} i_c}{V_{CC} I_C} \quad (24)$$

where P_{SW} is the switching losses, P_M is the losses in IGBT, P_D is the losses in diode, f_s is the switching frequency, and E_{onM}, E_{offM} and E_{onD} are the turn-on energy losses, trun-off energy losses and diode reverse-recovery energy losses respectively in the test condition of V_{CC} and I_{CC}. V_{CC} and I_{CC} are the collector-emitter voltage and collector current of insulated gate bipolar transistor (IGBT). Thus, only V_{ce} and i_c are changed during the switching operation.

Under the GFUP-PWM, the V_{ce} which is equal to V_{DM} is only changed between 0 and U_{dc}/2 in one switch period. However, due to the existence of dead zone between conduction mode and freewheeling mode, which is described in fig.2 (b), V_{ce} has two change processes which are from 0 to U_{dc} and U_{dc} to U_{dc}/2 in HFUP-PWM. Therefore, the switching losses of HFUP-PWM are more than two times as that in low frequency. Most of the time, the proposed hybrid UP-PWM method operates in low frequency as GFUP-PWM. Only in the compensation range of ZCD, θ, the HFUP-PWM is realized. Thus, the switching losses of hybrid modulation scheme are close to the GFUP-PWM.

TABLE I. PARAMETERS USED IN ANALYSIS AND SIMULATION

Parameters	Symbols	Values
Output power	P	4 kW
DC link voltage	U_{dc}	360 V
Grid voltage	V_g	220 V/rms
Grid frequency	f	50 Hz
Input DC capacitor	C_1	2800 μF
Filter inductor	L_1=L_2	1 mH
Switch frequency	f_s	20 kHz
Dead time	ε	1.5μs

III. SIMULATION RESULT

Simulation are carried out using Piecewise Linear Electrical Circuit Simulation (PLECS) to validate the feasibility of the proposed method. The main parameters are listed in Table 1. In order to achieve the simulation of the inverter efficiency, a thermal losses model of switches is established by the datasheet of insulated gate bipolar transistor (IGBT, Infineon IKW3N65EL5).

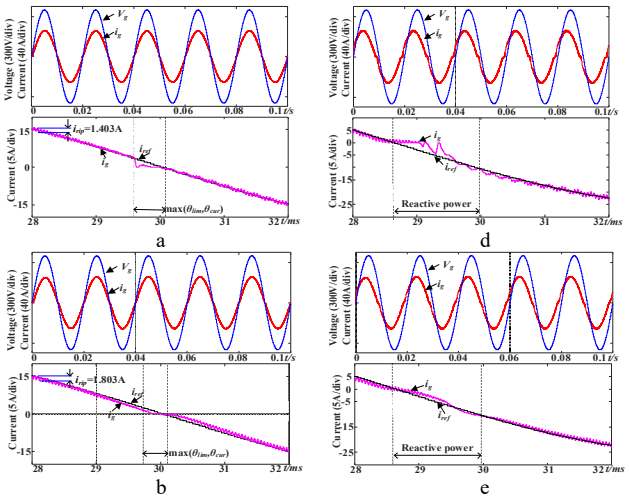

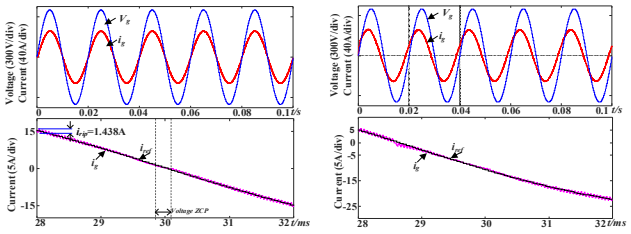

Fig. 6. Simulation results

a. GFUP-PWM at unity power factor
b. HFUP-PWM at unity power factor
c. hybrid UP-PWM at unity power factor
d. HFUP-PWM at non-unity power factor (cosφ=0.9)
e. hybrid UP-PWM at non-unity power factor (cosφ=0.9)

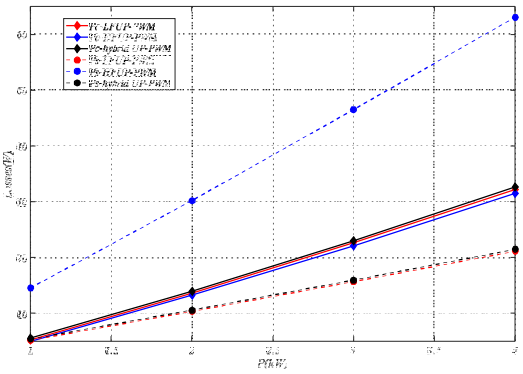

Fig. 7. Device losses comparision

Fig.6 shows comparison results at unity power factor and non-unity power factor (cosφ=0.9). The grid voltage V_g, the output current i_g, the reference current i_{ref} and ripple current i_{rip} are all displayed in every sub-graph. The waveforms of unity power factor in GFUP-PWM, HFUP-PWM and hybrid UP-PWM are sequentially shown in Fig 6. (a), (b) and (c), respectively. It is obviously that the ZCD in Fig.6 (c) is lower than that in Fig.6 (a) and (b). And the ripple current in Fig.6 (a), (b) and (c) are 1.403A, 1.803A and 1.438A, respectively. Through the Fast Fourier Transformation (FFT) analysis, the total current distortion rate (THD) are 2.38%, 3.06% and 1.61% in Fig.8 (a), (b) and (c). It is illustrated in Fig.6 that the power quality in proposed modulation is better than that of GFUP-PWM and HFUP-PWM.The Fig.6 (d), (e) and (f) show the results at non-unity power factor. It is showed in Fig.6 (d) that The current distortion under non-unity power factor is so serious that the GFUP-PWM has no reactive power capability. Besides, the ZCD problem in Fig.6 (e) is worse than that in Fig.6 (f). Moreover, the total current distortion rate (THD) are 3.27% and 2.01% in Fig.6 (a) and (b), respectively.

The simulation data of switching losses are displayed from 1kW to 4kW in Fig.7. The switching losses in proposed modulation are close to that in GFUP-PWM, and less than half of that in HFUP-PWM. And the conduction losses are almost the same in three modulation methods. The simulation results are consistent with theory analysis. All simulation results illustrate that the proposed hybrid UP-PWM for HERIC can achieve high efficiency and good power quality while provide reactive power support.

IV. Using the Template

In this paper, a hybrid UP-PWM for HERIC type inverter is proposed. The proposed method combines the advantages of GFUP-PWM, HFUP-PWM and the modulation of generating reactive power. When generating active power, it adopts GFUP-PWM. And only freewheeling switches act in high frequency when outputting reactive power. Those two modulation schemes can achieve low switching losses and ripple current. Besides, the paper utilizes HFUP-PWM near the voltage and current ZCPs. And the compensation of duty cycle and dead zone are added to remedy the defects which are caused by the narrow pulse limits and dead zones. The performances of the proposed hybrid UP-PWM, such as low switching losses, good power quality and reactive power capability, are verified by simulations and experimental results. Furthermore, the proposed modulation scheme can be extended other single-phase transformerless PV inverter topologies to achieve the same effects.

V. Acknowledge

This work was supported by the National Natural Science Foundation of China under Grant 61573384 and Grant 61622311, and the Fundamental Research Funds in the Central South University under Grant 2017zzts489.

References

[1] F. Blaabjerg, R. Teodorescu, M. Liserre, and A. Timbus, “Overview of control and grid synchronization for distributed power generation systems,” IEEE Trans. Ind. Electron., vol. 53, no. 5, pp. 1398–1409, Oct. 2006.

[2] W. Li, Y. Gu, H. Luo, et al. , “Topology Review and Derivation Methodology of Single-Phase Transformerless Photovoltaic Inverter for Leakage Current Suppression,” IEEE Trans. Ind. Electron., 2015, 62, (7), pp. 4537-4551

[3] Z. Guo and F. Kurokawa, “A novel PWM modulation and hybrid control scheme for grid-connected unipolar inverters,” in Proc. IEEE 26th APEC, Fort Worth, TX, 2011, pp. 1634–1641.

[4] DIN VDE 0126, “Automatic disconnection device between a generator and the public low-voltage grid,” Germany Standard, 2006, 2010.

[5] M. Victor, K. Greizer, and A. Bremicker, “Method of converting a direct current voltage from a source of direct current voltage, more specifically from a photovoltaic source of direct current voltage, into a alternating current voltage,” U.S. Patent 2005 028 6281 A1, Apr. 23, 1998.

[6] H. Schmidt, C. Siedle, and J. Ketterer, “Wechselrichter zum umwandeln einer elektrischen gleichspannung in einen wechselstrom oder eine wechselspannung”, EP Patent EP 1 369 985 A2, May 15, 2003.

[7] G. San, H. Qi, J. Wu, and X. Guo, “A new three-level six-switch topology for transformerless photovoltaic systems”, in Proc. IPEMC, 2012, pp. 163–166.

[8] B. Ji, J. Wang, and J. Zhao, “High-efficiency single-phase transformerless PV H6 inverter with hybrid modulation method”, IEEE Trans. Power Electron., vol. 5, no. 60, pp. 2104–2115, May 2013

[9] T. Wu, C. Kuo, H. Hsieh, “Combined unipolar and bipolar PWM for current distortion improvement during power compensation”, IEEE Trans. Power Electron., vol. 29, no. 4, pp. 1702-1709, April 2014.

[10] T. K. S. Freddy, J. H. Lee, H. C. Moon, K. B. Lee, and N. A. Rahim “Modulation technique for single-phase transformerless photovoltaic inverters with reactive power capability”, IEEE Trans. Ind. Electron., vol. 64, no. 9, pp. 6989-6999, Sep. 2017.

[11] F. Wu, B. Sun, K. Zhao, et al. “Analysis and solution of current zero-crossing distortion with unipolar hysteresis current control in grid-

connected inverter", IEEE Trans. Ind. Electron., vol. 60, no. 10, pp. 4450-4457, 2013.

[12] S. Deng, Y. Sun, J. Yang, et al. "Optimized hybrid modulation strategy for AC bypass transformerless single-phase photovoltaic inverters", Journal of Power Electronics, vol. 16, no. 6, pp. 2129-2138, 2016.

[13] VDE-AR-N 4105, "Power generation systems connected to the low-voltage distribution network-Technical minimum requirements for the connection to and parallel operation with low-voltage distribution networks", Verband der Elektrotechnik, Aug. 2011.

[14] G. Dušan, P. Marco, "IGBT power losses calculation using the data-sheet parameters", Handbook of Infineon Company, 2009, 1st edn., pp. 5–6.